MULTIMODAL ENERGY HARVESTING SKIN USING PIEZOELECTRIC UNIMORPH SHELL STRUCTURE

Soobum Lee[1], Byeng. D. Youn[2] *
[1] Department of Aerospace and Mechanical Engineering, Univ. of Notre Dame, Notre Dame, USA,
[2] School of Mechanical and Aerospace Engineering, Seoul National Univ., Seoul, Korea
* Corresponding author (bdiyoun@snu.ac.kr)

Keywords: *multi-modes, harmonic vibration, piezoelectric, voltage cancellation, inflection line*

1 Introduction

Energy harvesting (EH) research area has been emerged to build self-powered wireless electrical devices such as wireless sensors by collecting ambient or wasted energy. This EH technology is highly demanding because wireless sensors are increasingly used in the areas of structural health monitoring (SHM), building automation, and so on. The battery, a current power source for wireless sensors, can be troublesome due to their limited lifespan and replacement cost. This issue has motivated the rapid growth of the EH field.

Among various EH technology the studies of piezoelectric EH to utilize machine vibration have been focused on designing EH devices including shape [1-3] and electric circuit [4, 5], or both. Even though most piezoelectric EH devices take a form of cantilever, this form has some drawbacks from a practical point of view: (i) it requires an extra space because of a bulky proof mass and additional clamping part, (ii) it must be protected from dirt, moisture, and other environmental harms, and (ii) a great deal of vibration energy can be lost when clamping conditions become loosened after a long-time vibration. The disadvantages of the cantilever design motivated the proposition of an innovative and practical EH design entitled "energy harvesting skin (EHS) [6, 7]." In the EHS, thin piezoelectric patches were directly attached onto a vibrating shell structure to harvest electric power while attempting to overcome the drawbacks of the cantilever EH device.

This paper proposes an advanced EHS design concept, entitled *multimodal EHS*, which utilizes multimodal vibration and enhances the energy harvesting capability.

2 Design Rationale of Multimodal EH Skin

2.1 Voltage Cancellation Effect

This section explains the design rationale for the multimodal EHS. The design rationale consists of two major steps (See Fig. 1): design of piezoelectric material distribution and external resistors. First, topology optimization determines an optimal piezoelectric material distribution by removing the materials along inflection lines from multiple vibration modes. The layout of the inflection lines can be found using the voltage phase angle (See Section 2.1. for details). An additional shape optimization (SO) step can be performed to make smooth boundaries and enhance manufacturability. Second, after the material design, the external resistor values for each segment are additionally found for power maximization.

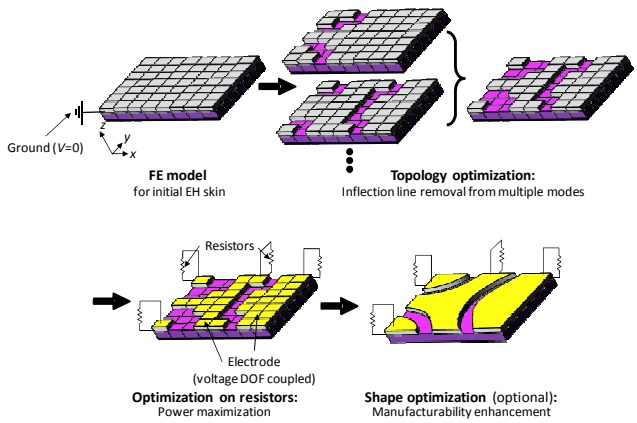

Fig.1. Prevention of cancellation effect by removing piezoelectric material at inflection points.

The finite element analysis is used for the design of multimodal EHS and the harmonic response analysis is considered [8], which solves the time-dependent equation of motion for linear structures under steady-state vibration. After solving this equation the complex electrical potential can be expressed in terms of maximum amplitude and phase angle:

$$\{V_{re}\}+i\{V_{im}\}=\{V_{\max}(\cos\phi+i\sin\phi)\}$$
$$V_{\max}=\sqrt{V_{re}^2+V_{im}^2},\qquad \phi=\tan^{-1}\frac{V_{im}}{V_{re}} \tag{1}$$

The objective of topological design proposed in this paper is to find the piezoelectric material distribution so that the voltage phase (ϕ in Eq. (1)) is almost identical in the material. Suppose the first three vibration modes are to be utilized for energy harvesting, using d_{31} effect. Because the generated voltage is proportional to the mechanical strain, the voltage cancellation occurs when the sign of mode-shape curvature changes [9]. Obviously this effect can be minimized by eliminating material around inflection points. Considering multiple modes in this example, the final design can be obtained as shown at the bottom of Fig. 2, by eliminating the material at all the inflection points from the second and the third mode. The same method can be applied in 3-dimensional skin vibration case.

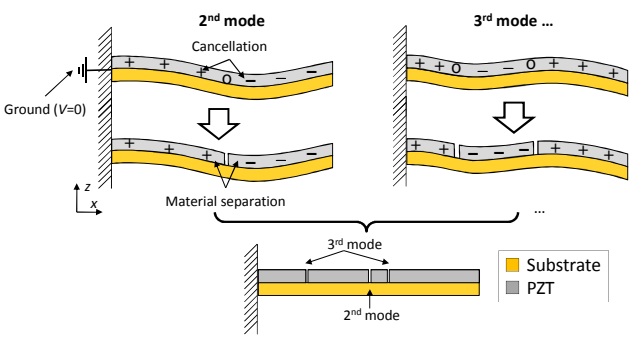

Fig. 2. Prevention of cancellation effect by removing piezoelectric material at inflection points.

The inflection line can be detected by voltage phase angle ($\phi(V)$) at each node at the top surface level of piezoelectric layer in Fig. 2. Usually a significant change on $\phi(V)$ exists across the inflection line (about 180°). An example of inflection line detection for a skin structure is shown in Fig. 3 which shows the top view (from positive z) of the EHS in Fig. 1. Suppose that an inflection line, the dotted line in Fig. 3, passes through the center of the element set. By this line the nodes at the top level are divided into two groups in terms of $\phi(V)$: $\phi\approx\theta$ on the right (void circles), $\phi\approx\theta+180°$ on the left (black circles). To detect and eliminate the inflection lines from multiple excitation frequencies (f_e^i, i is the mode index), the following procedure is performed:

- Step 1: Perform harmonic analysis for a single excitation frequency.
- Step 2: For ith excitation case, visit every FE node at top surface level of piezoelectric and extract the phase (ϕ).
- Step 3: For every top level node, check the phase difference with its neighboring 8 nodes
- Step 4: Extract the node set where the significant phase difference is detected (check marks in Fig. 3).
- Step 5: Eliminate the element set composed of the node set in Step 4.
- Step 6: Repeat Steps 1-5 for each excitation frequency.

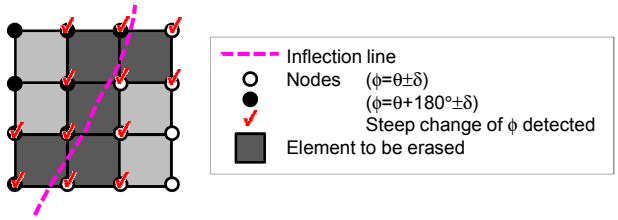

Fig. 3. Inflection line detection (top view of PZT elements)

3 Design Case Studies

To prove the excellent performance of the proposed multimodal EHS design method, two design case studies were researched: aircraft skin (Section 3.1) and power transformer (Section 3.2). For each case, two vibration modes are utilized for energy harvesting and about 30% power improvement has been achieved compared to the case where only one mode is utilized.

3.1 Utilization of Aircraft Skin Vibration

The multimodal vibration data from an aircraft skin (Fig. 4) was used for multimodal EHS design. This case study was motivated for the development of self-powered structural monitoring sensors for aircraft (e.g., for the detection of abnormal deformation of aircraft structure). The vibration level was measured 12 times and the fast Fourier Transformation (FFT) was performed to observe the multiple harmonic resonant peaks around 800 and 1500 Hz. In this case study these two resonant

frequency components were used for the design of multimodal EHS.

Fig. 4. Aircraft skin and measurement location

In this study a local part of aircraft skin (about 12.5×10.5 cm^2) was modeled. PZT patches were attached on the top of the aircraft skin (aluminum) to form a unimorph layout. The local model was defined as a rectangle with 9 rivet joints. The thicknesses of aluminum and PZT-5A are 1.6002 and 1.02 mm. The PZT patches and substrate were modeled using SOLID5 and SOLID45 element in ANSYS, respectively. Totally 6448 finite elements were used in this modeling.

The phase angle plots can be obtained through the harmonic response analysis for each excitation frequency (f_e^1 and f_e^2) as shown in Fig. 5(a). In both excitation cases the domain was clearly segmented. In f_e^1 excitation case, the vicinity of each rivet joint has positive phase while the other region (including the center of plate) has negative phase. In f_e^2 excitation case, however, the center segment was divided into two sub-regions. Fig. 5(b) shows the PZT layer segmentation by removing inflection lines from multiple modes.

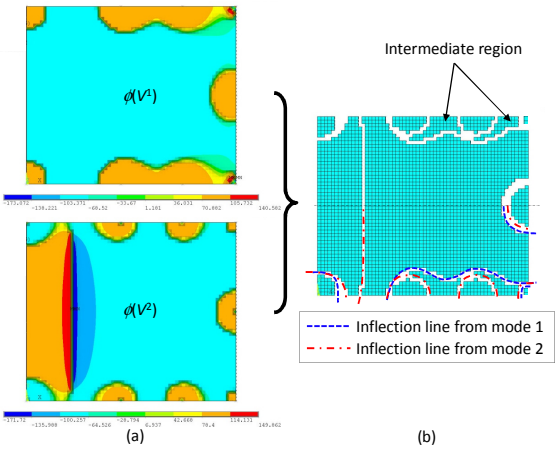

Fig. 5. (a) Voltage phase angles from multiple modes and (b) inflection line elimination

The shape optimization (SO) step was additionally performed as well as the optimization for external resistors. The parameterized model is shown in Fig. 6. The design parameters were defined in the lower half of the model and the model symmetry was assumed for the whole. In total 22 design variables were assigned in this design study. For more accurate simulation result, the FE model was refined with 14598 elements in total.

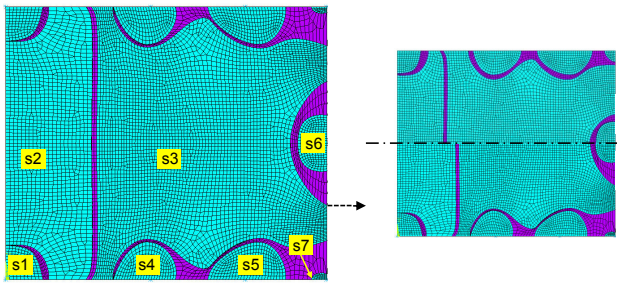

Fig. 6. Design optimization result and comparison with initial model

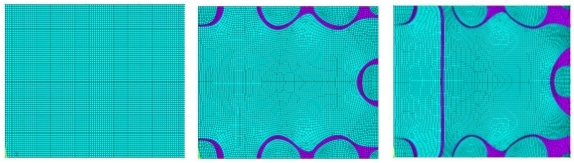

(a) (b) (c)

Fig. 7. Multimodal EHS with different segmentation: (a) Case 0 (b) Case 1 (unimodal EHS) (c) Case 2 (multimodal EHS)

The performance improvement of the multimodal EHS was summarized in Table 1 in which the power generation per unit acceleration (1g) was compared for the three different cases (also see Fig. 7): no segmentation (Case 0), segmentation considering the first mode only (Case 1, entitled "unimodal EHS"), and multimodal EHS (Case 2). Rows (i) and (ii) indicate the power generation when each case is excited at f_e^1 and f_e^2 frequency, respectively. The more segmentation we implement according to the design rule suggested in this paper, the larger power the EHS generated as shown in Table 1. When the design is evolved from Case 0 to Case 1, the power level increased significantly for the both modes (22.2 and 33.8%). It is analyzed that the segmentation near the fixed rivet joints contributes to the power improvement at both modes. When Case 1 and Case 2 are compared, the power is mainly increased at second mode (29.7%). It

indicates that the elimination of the vertical inflection line (across the width of the skin) mainly contributes to power increase for the second mode. In summary, greater power generating performance of the multimodal EHS (Case 2) was clearly proven.

Table 1 Power comparison for different segmentation

		(a)	(b)	(c)
Power / accel. (mW/g)	(i) at f_e^1	1.479	1.807	1.836
	(ii) at f_e^2	0.136	0.182	0.236

3.2 Utilization of Power Transformer Vibration

The second case study involved a power transformer vibration. The alternating magnetic field causes fluctuating electromagnetic forces in the windings (see Fig. 8) and they produce harmonic vibration in the transformer.

The finite element model for the transformer has been constructed using ANSYS as shown in Fig. 8. This figure shows the FE model composed of internal 3 windings, supporting structures, and exterior walls with radiation ribs. The dimension of the transformer is 0.69×1.13×1.65m^3. The transformer walls are 15 mm thick, made of cast steel. Copper was chosen for the material property of the windings. Totally 27972 SOLID45 element were used for the modeling. The fixed boundary condition was applied at the bottom surface of the transformer.

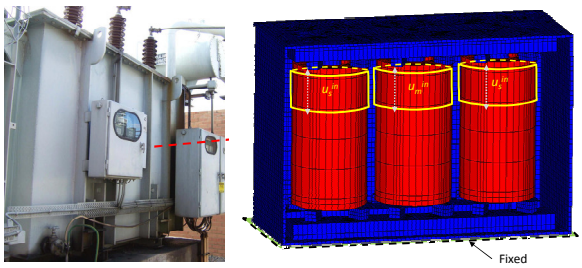

Fig. 8. Design of multimode EHS on a power transformer wall

The multimodal EH skin design task introduced in Section 2 was applied to the transformer. The PZT-5A patches (1.02mm thick) covering the front panel were modeled using SOLID5 element in ANSYS. The volt DOFs on the interface with the transformer panel were grounded. The voltage coupling condition at the exterior surface (representing exterior electrode) and the external resistors were implemented after eliminating inflection lines.

Fig. 9 shows the PZT layer segmentation by removing inflection lines. Fig. 9(a) shows the unimodal EH skin design (only the f_e^1 excitation case was considered), whereas the multimodal EH skin design was displayed in Fig. 9(b) (both f_e^1 and f_e^2 excitation cases were considered). In this stage, at each segment, the voltage DOFs for the nodes on the exterior PZT surface were coupled to represent an electrode. CIRCU94 element was used to represent electrical resistors.

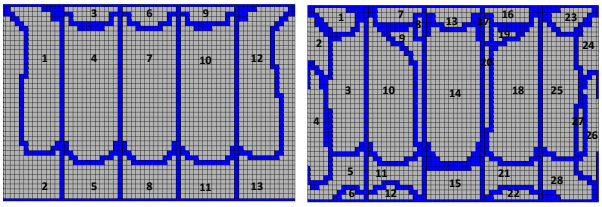

(a) unimodal EHS (b) multimodal EHS

Fig. 9. Design of multimode EHS on a power transformer wall

The amount of energy harvested from each design is analyzed in Table 2. Basically the unimodal design harvests more power from the first mode (8.00mW) rather than the multimodal design (7.80mW). Based on the fact that less amount of PZT was used in the multimodal design, however, the performance of multimodal skin under the first mode excitation is still comparable. Moreover the advantage of the multimodal design is clearly shown from the second mode. Compared with the unimodal design (2.98mW), 81% increase of power was harvested in the multimodal design (5.38mW). For the total power the multimodal design harvests 13.18mW, about 20% larger than the unimodal design (10.98mW). To summarize, the excellent power generating performance of multimodal EH skin was clearly proven.

The power improvement by the multimodal EH skin design can facilitate larger number of wireless sensor operation. Considering the power requirement of a 3-axis wireless accelerometer (2.4mW [10]), we can expect the multimodal design can operate five accelerometers. The larger number of sensors will enhance the detectability of the failure modes in the transformer and enable high-reliability structural health monitoring and life

prognostics. In practice the segments with small power generation in the multimode design (e.g., segment 6, 8, 17, 19, 27) can be removed to save the material.

Table 2. Comparison of power

Design	Unimodal		Multimodal	
Mode	1	2	1	2
Power (mW)	8.00	2.98	7.80	5.38
	10.98		13.18	

4 Conclusion

The new EH design concept, multimodal energy harvesting skin (EHS), was proposed for power generation from multiple harmonic vibration modes. The topological design of the multimodal EHS was obtained by removing the PZT material along the inflection lines from multiple modal shapes, in order to minimize the cancellation effect. The optimal external resistors at all segments were found using design optimization algorithm for power maximization. The multimodal EHS was compared with the skin without segmentation and the unimodal EHS, and the superior performance of the multimodal EHS was verified. Additional shape optimization may be followed for better manufacturability.

The proposed design principle for the multimodal EHS can be successfully applied to a plenty of engineered systems which have harmonically vibrating skins. In the near future we plan to prove the versatility of the design concept with applications including structural health monitoring, building automation, etc. by integrating multimodal EHS and wireless sensors.

References

[1] P. Glynne-Jones, S. P. Beeby, and N. M. White, "Towards a piezoelectric vibration-powered microgenerator," *IEE Science, Measurement and Technology,* vol. 148, pp. 68-72, 2001.

[2] F. Goldschmidtboeing and P. Woias, "Characterization of different beam shapes for piezoelectric energy harvesting," *Journal of Micromechanics and Microengineering,* vol. 18, p. 104013, 2008.

[3] S. Roundy, E. S. Leland, J. Baker, E. Carleton, E. Reilly, E. Lai, B. Otis, J. M. Rabaey, P. K. Wright, and V. Sundararajan, "Improving power output for vibration-based energy scavengers," *Pervasive Computing, IEEE,* vol. 4, pp. 28-36, 2005.

[4] A. Kasyap, J. Lim, D. Johnson, S. Horowitz, T. Nishida, K. Ngo, M. Sheplak, and L. Cattafesta, "Energy reclamation from a vibrating piezoceramic composite beam," in *the Ninth International Congress on Sound and Vibration (ICSV9)*, 2002.

[5] G. K. Ottman, H. F. Hofmann, A. C. Bhatt, and G. A. Lesieutre, "Adaptive piezoelectric energy harvesting circuit for wireless remote power supply," *Power Electronics, IEEE Transactions on,* vol. 17, pp. 669-676, 2002.

[6] S. Lee and B. D. Youn, "A new piezoelectric energy harvesting design concept: multimodal energy harvesting skin," *Ultrasonics, Ferroelectrics and Frequency Control, IEEE Transactions on,* vol. 58, pp. 629-645, 2011.

[7] S. Lee and B. D. Youn, "A design and experimental verification methodology for an energy harvester skin structure," *Smart Materials and Structures,* vol. 20, pp. 057001, 2011.

[8] H. Allik and T. J. R. Hughes, "Finite element method for piezoelectric vibration," *International Journal for Numerical Methods in Engineering,* vol. 2, pp. 151-157, 1970.

[9] S. Lee, B. D. Youn, and B. C. Jung, "Robust segment-type energy harvester and its application to a wireless sensor," *Smart Materials and Structures,* vol. 18, pp. 095021, 2009.

[10] "Analog temperature sensor," in *Ambiosystems LLC*. vol. 2008.